PCCP

RSC Publishing

PAPER

Microlens array induced light absorption enhancement in polymer solar cells

Cite this: *Phys. Chem. Chem. Phys.*, 2013, **15**, 4297

Yuqing Chen,[a] Moneim Elshobaki,[bc] Zhuo Ye,[de] Joong-Mok Park,[de] Max A. Noack,[f] Kai-Ming Ho[de] and Sumit Chaudhary*[ab]

Over the last decade, polymer solar cells (PSCs) have attracted a lot of attention and highest power conversion efficiencies (PCE) are now close to 10%. Here we employ an optical structure – the microlens array (MLA) – to increase light absorption inside the active layer, and PCE of PSCs increased even for optimized devices. Normal incident light rays are refracted at the MLA and travel longer optical paths inside the active layers. Two PSC systems – poly(3-hexylthiophene-2,5-diyl):(6,6)-phenyl C61 butyric acid methyl ester (P3HT:PCBM) and poly[[9-(1-octylnonyl)-9H-carbazole-2,7-diyl]-2,5-thiophenediyl-2,1,3-benzothiadiazole-4,7-diyl-2,5-thiophenediyl]:(6,6)-phenyl C71 butyric acid methyl ester (PCDTBT:$PC_{70}BM$) – were investigated. In the P3HT:PCBM system, MLA increased the absorption, absolute external quantum efficiency, and the PCE of an optimized device by ~4.3%. In the PCDTBT:$PC_{70}BM$ system, MLA increased the absorption, absolute external quantum efficiency, and PCE by more than 10%. In addition, simulations incorporating optical parameters of all structural layers were performed and they support the enhancement of absorption in the active layer with the assistance of MLA. Our results show that utilizing MLA is an effective strategy to further increase light absorption in PSCs, in which optical losses account for ~40% of total losses. MLA also does not pose materials processing challenges to the active layers since it is on the other side of the transparent substrate.

Received 22nd January 2013,
Accepted 22nd January 2013

DOI: 10.1039/c3cp50297j

www.rsc.org/pccp

Introduction

In this era of depleting fossil-fuel based energy sources, and their environmental impact, focus on renewable energy sources is becoming increasingly important. Direct conversion of solar energy to electricity is very attractive due to the abundance of solar energy resource, which dwarfs all other energy resources combined. Within the solar cell community, polymer-based solar cells (PSCs) have received heightened attention due to advantages such as flexibility, potentially low cost production, light weight and easy integrability into building products, clothes and fabrics. PSCs have been making rapid progress in research and development in academia and industry; maximum power conversion efficiencies (PCE) have increased from around 2% to 10% in the last decade.[1,2] This progress is owing to the development of new materials, and novel device structures and processing conditions. So far, the majority of studies on PSCs have focused on the development of new materials,[3–5] interlayers,[6–8] and morphology optimisation.[9–13] Another important way to enhance the PCE of PSCs is by increasing light absorption inside the active layers using various optical approaches. Enhancing light absorption is important because active layers in PSCs are quite thin, which leads to optical losses accounting for ~40% of total losses.[14] In true bilayer donor–acceptor heterostructures, active layers can only be ~10 nm thick due to short exciton diffusion lengths (around 5–10 nm[15]). On the other hand, in bulk-heterojunction structures, in which the donors and acceptors are intimately mixed together in a single layer, higher thickness can be afforded. However, such thicknesses (~100–200 nm, at times less) are still not enough to efficiently absorb light, and thicknesses cannot be indiscriminately increased further because of low charge carrier mobilities in most organic materials. Hence, to boost efficiencies further, it is imperative to improve light absorption within existing PSC architectures.

Some optical approaches enabling light trapping in PSCs have been proposed and implemented. These include approaches

[a] *Department of Electrical and Computer Engineering, Iowa State University, Ames, IA, USA. E-mail: sumitc@iastate.edu; Tel: +1 515 294 0606*
[b] *Department of Materials Science and Engineering, Iowa State University, Ames, IA, USA*
[c] *Faculty of Science, Physics Department, Mansoura University, Mansoura 35516, Egypt*
[d] *Ames Laboratory-USDOE, Iowa State University, Ames, IA, USA*
[e] *Department of Physics and Astronomy, Iowa State University, Ames, IA, USA*
[f] *Microelectronics Research Center, Iowa State University, Ames, IA, USA*

like textured substrates,[16] wrinkles and deep folds,[17] metal nanospheres,[18,19] and microlens arrays.[20] However, these methods suffer from one or more weaknesses. In the case of textured substrates, topographical dimensions of textures (gratings) need to be designed optimally to enable a conformal coating of active layers. High aspect-ratio gratings can result in shunts between top and bottom electrodes, underfilling, and air gaps inside active layer film.[16] Whereas, narrow pitch gratings lead to overfilling of trenches and increased losses from carrier recombination.[16] Another challenge is that for different polymer systems with different optimum active-layer thicknesses, grating dimensions need to be redesigned and retested for conformal polymer coating. The approach of utilizing substrates with wrinkles and deep fold features suffers from similar issues. Besides, it is challenging to have a quantitative and precise control on the dimensions of self-assembled wrinkles and folds. Utilizing metal nanospheres inside active layers employs plasmonic near-field enhancement effects to trap more light. However, this approach also has drawbacks such as inclusion of metallic and surface group impurities, which could act as recombination centers and degrade charge transport. Utilizing a microlens array (MLA), as an additional structure on the side of the transparent substrate opposite to the active-layer, is another approach to increase light absorption inside the active layer of PSCs. Since MLA is located on the other side of the substrate, this approach is non-intrusive in nature, and has no effect on the device fabrication processing or internal morphology of the active-layer. It has also been demonstrated as a universal method of light absorption enhancement in different organic photovoltaic systems.[20] In this previous demonstration, MLA consisted of hemispherical microlenses with a diameter of 100 μm. These 100 μm microlenses reduce surface-reflection, and refract the incoming light towards the active layer, thus increasing the optical path. In this study, we utilized the near-hemispherical microlenses of 2 μm diameter. With a sharper peak, the near-hemispherical shape is better than a pure-hemispherical shape towards refracting incoming light. These microlenses, with diameter close to visible light wavelength, not only reduce surface reflection and refract incoming light like 100 μm microlenses, but also utilize optical interference to enhance light intensity inside the active layer. Even though 100 μm MLAs act as gratings, the diffraction angles are small, which makes the diffraction small and hard to observe. However 2 μm MLAs have a period closer to visible light wavelength, which makes the diffractive angles larger than that of 100 μm MLAs. Thus we expected that the more diffractive nature of the 2 μm period compared to the 100 μm period will make the light enhancement in 2 μm MLAs higher. This is indicated by simulations on MLAs with diameters of 2 μm and 6 μm. Since 6 μm is much larger than visible light wavelength (short wavelength limit), light absorption in the PSCs can be studied with geometrical optics, or ray optics, where optical effects such as diffraction and interference are not accounted for (the diffraction effect is very small as discussed above). In this short wavelength limit, the 6 μm and 100 μm MLAs yield the same light absorption enhancement. We show these simulation results in the simulation section of this paper. We fabricated two types of PSCs on our MLA substrates and compared their performance with devices without MLA. Performance enhancement in MLA devices is demonstrated in the following sections through different characterizations and discussion.

Methods and experimental

Microlens array

The MLA is composed of arrays of microlenses as shown in Fig. 1. Microlenses were near-hemispherical with a diameter of 2 μm, and they sit on the side of a glass substrate facing the incident light. The array is fabricated by imprinting a polydimethylsiloxane (PDMS) mold on a UV curable polyurethane (PU) drop placed on the glass. More details about fabrication of MLA on glass are described elsewhere.[21]

P3HT:PCBM PSC system

P3HT (Solarmer Inc.) and PCBM (Nano-C Inc.) were dissolved in 1,2-dichlorobenzene (*o*-DCB) with 20 mg ml^{-1} concentration for each and stirred at 800 rpm on a hot plate at a temperature of 45 °C for around 20 hours to make active layer solution. Indium Tin Oxide (ITO) coated glass (Delta Technologies) and ITO coated glass with the MLA pattern were ultrasonicated in 2-propanol/acetone, and de-ionized water, respectively, for 2 minutes. Then both substrates were dried with nitrogen and exposed to air plasma for 1 minute. Poly(3,4-ethylenedioxythiophene):poly(styrenesulfonate) (PEDOT:PSS) was spin-coated on the ITO side of the glasses at 3000 rpm for 60 s. Spin-coated devices were annealed on a hot plate at 100 °C for 10 minutes. Both substrates were then transferred inside a glovebox filled with nitrogen. The previously prepared active layer solution was filtered through a 0.2 μm filter. Filtered solution was dropped on the PEDOT:PSS film devices and spun at the speed of 500 rpm for 45 seconds, to yield an active layer thickness of around 200 nm. After spin-coating, devices were covered under separate petri dishes for 1 hour. This amount of time is long enough to dry the active layer and its color changes from orange to dark purple. Devices were then taken out from petri dishes and annealed on a hot plate at 110 °C for 10 minutes. After annealing, devices were transferred to a thermal evaporator with loaded calcium (Ca) and aluminum (Al) sources. Under a vacuum level of around 10^{-6} mbar, 25 nm of Ca was evaporated on the active layer, followed by 100 nm of Al layer. Following the same fabrication process, six cells were fabricated in one batch. In total, two batches were fabricated.

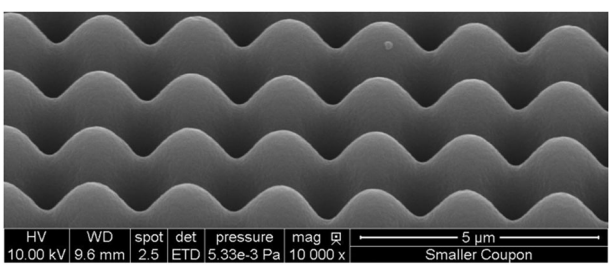

Fig. 1 SEM image of the PU layer with the MLA pattern.

PCDTBT:P_{70}CBM PSC system

PCDTBT of molecular weight 50 kDa was purchased from 1-material. MoO_X (99.99%), LiF (99.98%) and $PC_{70}BM$ were purchased from Sigma Aldrich. For the PCDTBT:$PC_{70}BM$ system, 10 nm of MoO_X anode buffer layer was thermally evaporated on ITO under a vacuum of about 10^{-6} mbar at a rate 0.5 Å s^{-1}. A solution of PCDTBT and $PC_{70}BM$ (weight ratio 1 : 3.5), with a concentration of 7 mg mL^{-1} in dichlorobenzene (DCB) was kept stirring on a hot plate at 90 °C and 650 rpm for eight hours. After that, the temperature of the solution was reduced to 60 °C at the same stirring speed. After several days, the active layer was spin coated on the top of the MoO_X layer at 2000 rpm for 45 seconds. The devices were dried under petri dish for 20 min, and then annealed for 15 min on a hot plate at 70 °C. Finally, LiF (2 nm) and Al (130 nm) were thermally evaporated over the active layer with a shadow mask of area 0.1256 cm^2 with an evaporation rate of less than 0.5 and 8 Å s^{-1}, respectively. Following the same fabrication process, six cells were fabricated in one batch, and a total of three batches were fabricated.

Characterization

Several characterizations were carried out as described below. Current–voltage characterization was done using the ELH Quartzline halogen lamp at 1 sun intensity, which was calibrated using a reference crystalline Si solar cell coupled with a KG-5 filter. Absolute external quantum efficiency (EQE) was determined using a custom setup built from a single grating monochromator (Horiba Jobin Yvon Srl), 100 W halogen bulb (OSRAM Bellaphot), and a current preamplifier (Ithaco, Inc.). An optical chopper (Thor Labs) coupled with a lock-in amplifier (Stanford Research Systems) were also used to reduce noise in the system. EQE was carried out at room temperature in the presence of ambient light. For absorption characterization, ITO coated glasses were deposited with PEDOT:PSS (for the P3HT system) or MoO_X (for the PCDTBT system) and an active layer following the fabrication process in the previous sections. Then these active-layer coated substrates were optically characterized using a Varian Cary 5000 UV-Vis-NIR spectrophotometer. Global reflection and global transmission were obtained from the spectrophotometer. Then absorption was calculated using 100% subtracting global reflection and global transmission.

Results and discussion

We chose to investigate the P3HT:PCBM system because it is the most widely investigated system in the field of PSCs. Even though new promising materials have emerged recently, P3HT:PCBM systems remain relevant for one of the sub-cells in tandem structures. Illustrated in Fig. 2(a) is a conventional P3HT:PCBM device, which is our control device in this study. The corresponding P3HT:PCBM device with an additional layer of MLA on one side of glass (called the MLA device) is schematically shown in Fig. 2(b). The performance parameters of current–voltage characterization of the two devices are listed in Table 1. The performance parameters of each device in the table are averaged from six cells in one batch. Since the devices were fabricated under optimized conditions from our experience and through the literature, it can be observed that even the control device has a quite high PCE of around 4.69%, one of the highest among P3HT:PCBM devices in the literature. The performance of the MLA device increases by 4.3% to 4.89%. This improvement is due to enhancement of current density (J_{sc}), which increases from 11.78 mA cm^{-2} in the control device to 12.19 mA cm^{-2} in the MLA device. The performance enhancement in percentage is not as high in our case as in the previous P3HT:PCBM study with 100 μm microlenses.[20] However, it should be noted that our fabrication conditions are more optimized, and even our control P3HT:PCBM device performs better than the MLA P3HT:PCBM device in that study.

In Fig. 3(a), the MLA device shows higher absolute EQE than the control device in the wavelength between 400 nm to 800 nm. From a quantitative view of this enhancement as in Fig. 3(c), the enhancement from the MLA reaches up to 5% in the shorter wavelength range below 600 nm, while in the wavelength range above 600 nm the enhancement can be as high as 20%. Since the MLA layer is on the separate side of the glass substrate from device structure, the microlenses do not affect the process of exciton diffusion/dissociation, charge transport and collection. However, the MLA layer can change the direction and distribution of incoming light in the active layer. Incoming light beams get refracted through MLA and have longer optical paths compared to those without MLA.

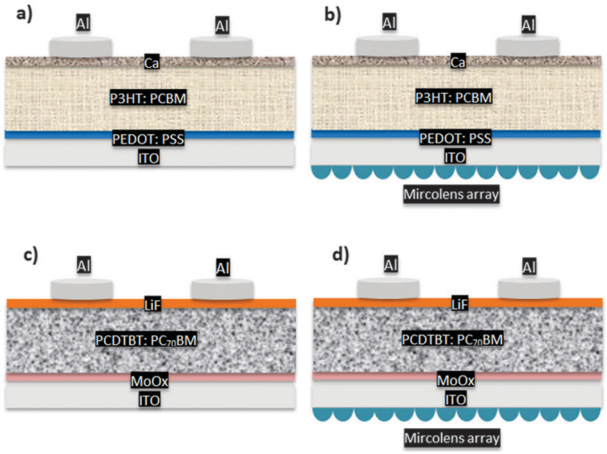

Fig. 2 Schematic structures of different PSC systems: P3HT:PCBM system (a) without MLA and (b) with MLA; PCDTBT:$PC_{70}BM$ system (c) without MLA and (d) with MLA.

Table 1 Parameters of current–voltage characterization of two PSC systems with and without 2 μm MLA

	P3HT:PCBM				PCDTBT:$PC_{70}BM$			
System parameters	J_{sc} (mA cm^{-2})	PCE	V_{oc} (V)	FF	J_{sc} (mA cm^{-2})	PCE	V_{oc} (V)	FF
Control	11.78	4.69%	0.60	66%	12.75	5.6%	0.88	50%
MLA	12.29	4.89%	0.60	66%	14.12	6.4%	0.88	51%
Enhancement	4.3%	4.3%	0%	0%	10.7%	14.3%	0%	2%

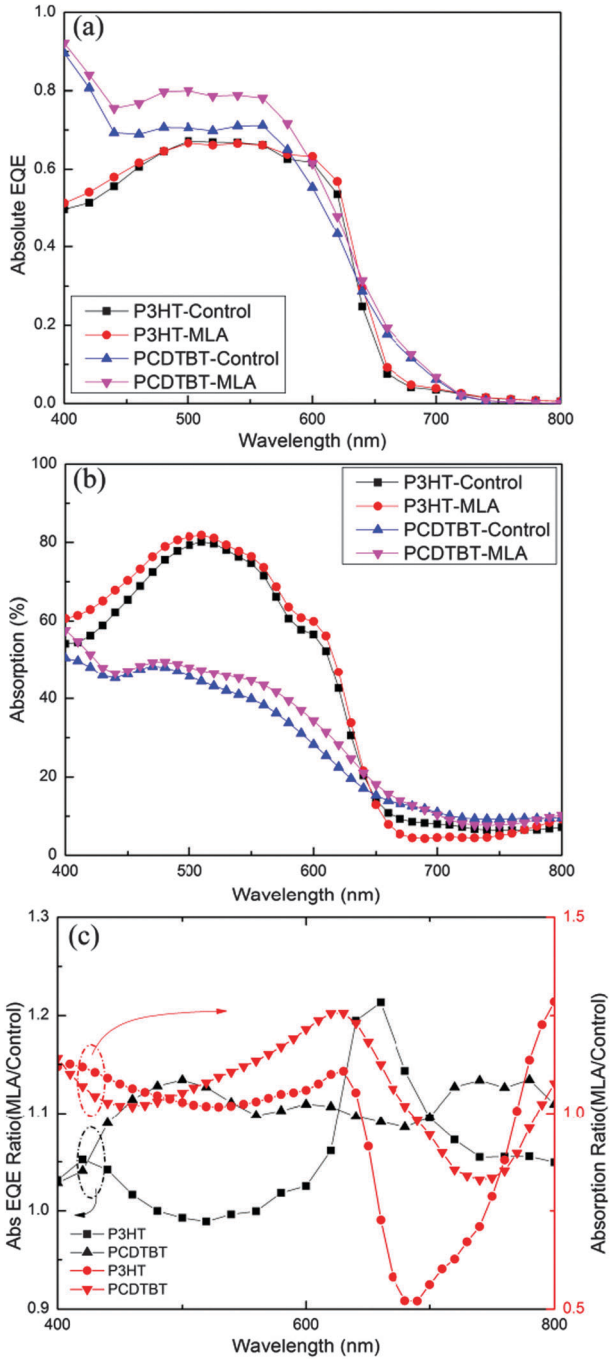

Fig. 3 (a) Absolute EQE of P3HT:PCBM and PCDTBT:$PC_{70}BM$ devices without (control) and with (MLA) MLA. (b) Absorption of P3HT:PCBM and PCDTBT:$PC_{70}BM$ devices without (control) and with (MLA) MLA. (c) Abs EQE ratio of MLA device to control device (black color); absorption ratio of MLA device to control device (red color).

Longer paths give light more chance to be absorbed inside the active layer. Besides, light beams, which get reflected on one microlens would encounter another neighbouring microlens and get refracted into the active layer, thus reducing surface reflection. At the same time, a close-packed MLA with diameter 2 μm close to visible light wavelength acts as a structured grating to produce a diffraction pattern inside the active layer. This diffraction would enhance light intensity inside the active layer, contributing to more exciton creation and hence charge carriers. The light absorption spectra inside the active layer of P3HT:PCBM devices are measured and depicted in Fig. 3(b). As shown in Fig. 3(c), between wavelengths 400 nm and 650 nm, MLA leads to broadband enhancement of light absorption inside the active layer, with the highest enhancement up to 10%. In the wavelength range between 650 nm and 780 nm, there is reduction in light absorption in the MLA device compared to the control device. It may be caused by light interference in this wavelength region, which reduces light intensity inside the active layer. However the light absorption in this range is far smaller than that below 650 nm. This little reduction of light absorption does not significantly change the total light absorption enhancement. Thus, it can be seen that by simply adding a MLA layer on the glass substrate, the P3HT:PCBM device gets more light absorption in the active-layer, leading to higher current density and PCE.

In PCDTBT:$PC_{70}BM$ devices, with similar structure and same function of MLA in PSC devices, we expected that the light absorption, absolute EQE and the current density will also increase. In fact, we expected higher enhancement because PCDTBT:$PC_{70}BM$ active layers are only 70 nm thick in optimized devices.[22] In order to verify our hypothesis, the similar characterization of the PCDTBT:$PC_{70}BM$ system as the P3HT:PCBM system was carried out. From Table 1 it is clear that the short circuit current density is enhanced by 10.7%, and PCE is increased from 5.6% to 6.4%. The spectra of the absolute EQE in Fig. 3(a) also clearly show an enhancement in the case of the MLA device, supporting the current density enhancement. In the wavelength region between 450 nm to 800 nm, the enhancement of EQE is slightly larger than 10% as seen in Fig. 3(c). The light absorption spectra, shown in Fig. 3(b) also support our expectation about the effect of the MLA. The light absorption inside the active layer is enhanced from MLA in the entire region between 400 nm and 700 nm, except for a little reduction between 700 nm and 800 nm. As seen in Fig. 3(c), between 400 nm and 550 nm, the enhancement falls below 10%. The enhancement between 550 nm and 650 nm becomes higher than 10% and reaches a maximum of 26% at 625 nm.

The existence of the diffraction effect from MLA is demonstrated in Fig. 4. The measurement was carried out on a surface. On the surface there was a hole, which was larger than PSC devices.

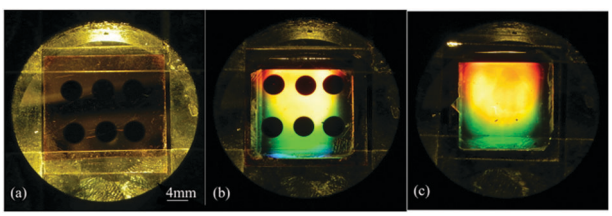

Fig. 4 Optical photos taken above devices with light of halogen lamp shining through devices from the bottom. (a) Control device without MLA, (b) MLA device with MLA, and (c) ITO coated glass with MLA.

One halogen lamp was put just under the hole at some distance so that light can shine through the hole. Three devices with a P3HT:PCBM active layer: control device, MLA device, and ITO coated glass with MLA were put above the hole in turn experiencing the same light conditions. Then optical photos were taken from above the devices using a digital camera with the same setup. The control device, which has no MLA layer, shows conformal light mapping as seen in Fig. 4(a). However, Fig. 4(b) and (c) show diffraction patterns in a device with MLA and glass with MLA, respectively. Microlenses behave like small diffraction gratings on the micrometer scale, which generate colourful mapping from the visible light. Thus the combination of hundreds of small diffraction gratings obviously forms diffraction and interference patterns inside the active layer as well, thus further increasing the effective optical path. The enhanced light intensity contributes to more exciton creation and charge carriers inside the active layer. The above colourful mappings on the surface are for substrates with 2 μm MLA, obviously showing the diffraction effect. However the substrate with 100 μm MLA did not show the colourful mapping on the device surface (not shown here in this paper). Even though 100 μm MLA is a periodical grating structure, the diffractive angle is very small since the period is far larger than visible wavelength. So there is barely any diffraction effect observed in 100 μm MLA devices. With the MLA grating period reduced to 2 μm, the diffractive angle increases and shows a diffraction effect as seen in the colourful mapping. Thus, the 2 μm MLA enhances more light absorption than the 100 μm MLA.

In summary, MLA brings enhancement in these two PSC systems. Because the thickness of the active layer in P3HT:PCBM (around 200 nm) is far larger than that in PCDTBT:$PC_{70}BM$ (around 70 nm), the light absorption in the first system is already high enough while the light absorption in the second system is lower. So the light absorption enhancement effect of the MLA in the second system is more prominent than that in the first system. This indicates that MLA is an effective way to enhance light absorption in PSC systems, especially when light absorption in the original device is not very high.

Simulation

Light absorption simulation is done for both PSC systems with both control and MLA devices as shown in Fig. 5(a). The simulation of these devices is based on the structures in Fig. 2. The planewave-based transfer matrix method[23–25] is applied as a full-field electromagnetic approach to obtain the absorption spectrum. In the simulation, the wavelength range is restricted to 400 nm to 800 nm to match the solar spectrum and the two PSC systems' absorption. Optical parameters such as refractive indices n and the extinction coefficients k are obtained from the literature.[26–29] Fig. 5(a) shows the simulated absorption for both PSC systems with control and MLA devices, revealing the higher absorption in MLA devices than that in control devices. In the wavelength range between 400 nm and 650 nm, where most of the light was absorbed for P3HT devices, the light absorption in the MLA device shows

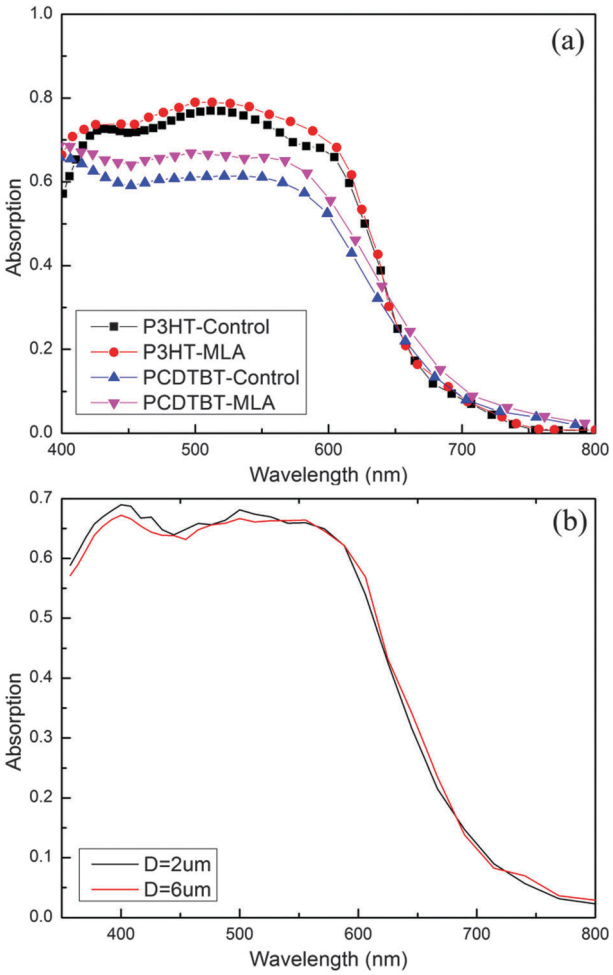

Fig. 5 (a) Simulation of light absorption inside active layers of P3HT:PCBM and PCDTBT:$PC_{70}BM$ devices without (control) and with (MLA) MLA. (b) Absorption simulation spectra of PCDTBT:$PC_{70}BM$ devices with MLA of diameters 2 μm and 6 μm.

enhancement as large as 10% around 400 nm and 570 nm, with an average improvement of around 4% compared to the control device. The simulated light absorption of PCDTBT devices experiences average of 9% enhancement in the MLA device than the control device between light wavelength of 400 nm and 650 nm. In order to confirm our expectation of higher light absorption with 2 μm MLA than that with 100 μm MLA, simulation with both 2 μm MLA and 6 μm MLA is employed and shown in Fig. 5(b). MLA with diameter 6 μm is far larger than visible light wavelength, which only plays a ray optic effect to increase the light optical path inside the active layer, similar to MLA with diameter 100 μm. Below 600 nm, the absorption spectra show an average of 4% higher absorption in 2 μm MLA than in the case of 6 μm MLA, where most of light absorption happens. From these simulations, we can more confidently say that employing 2 μm microlens arrays is a more effective way to enhance the performance of PSCs, than MLAs with much greater dimensions. Of course, 2 μm might not be the most optimal dimension and in the vicinity of these dimensions, there might be one that can perform better. That exploration is a part of our current and future studies.

Conclusions

In this work, two types of PSC systems: P3HT:PCBM and PCDTBT:$PC_{70}BM$ are investigated with a 2 μm microlens array on one side of the glass substrate. Devices with MLA have a better performance than that without MLA. In the P3HT:PCBM system, MLA increases the absorption, absolute external quantum efficiency, and PCE by 4.3%, even for a conventional device with fabrication conditions optimized for high efficiency. In the PCDTBT:$PC_{70}BM$ system, MLA increases the absorption, EQE and PCE by more than 10%. All of these enhancements are due to the increased light path and absorption inside the active layer from refracted light through the microlens as well as diffraction induced light intensity enhancement. This improvement of light absorption is further supported by simulations in the two PSC systems. Our MLA approach is more effective in devices with a thinner active layer than that with a thicker active layer. MLAs also do not pose materials processing challenges to the active-layers since they are on the other side of the transparent substrate.

Acknowledgements

SC acknowledges National Science Foundation for financial support (Award # CBET – 1236839). Y. Chen thanks financial assistance from Chinese Scholarship Council (CSC). M. Elshobaki thanks financial support from the Egyptian Government.

Notes and references

1 Z. He, C. Zhong, S. Su, M. Xu, H. Wu and Y. Cao, *Nat. Photonics*, 2012, **6**, 593–597.
2 NREL, Best Research Cell Efficiency Records, http://www.nrel.gov/ncpv/images/efficiency_chart.jpg.
3 D. Gendron and M. Leclerc, *Energy Environ. Sci.*, 2011, **4**, 1225–1237.
4 S. Günes, H. Neugebauer and N. S. Sariciftci, *Chem. Rev.*, 2007, **107**, 1324–1338.
5 R. Kroon, M. Lenes, J. C. Hummelen, P. W. M. Blom and B. de Boer, *Polym. Rev.*, 2008, **48**, 531–582.
6 H.-L. Yip and A. K. Y. Jen, *Energy Environ. Sci.*, 2012, **5**, 5994–6011.
7 E. L. Ratcliff, B. Zacher and N. R. Armstrong, *J. Phys. Chem. Lett.*, 2011, **2**, 1337–1350.
8 R. Po, C. Carbonera, A. Bernardi and N. Camaioni, *Energy Environ. Sci.*, 2011, **4**, 285–310.
9 J. A. Carr, Y. Chen, M. Elshobaki, R. C. Mahadevapuram and S. Chaudhary, *Nanomater. Energy*, 2011, **1**, 18–26.
10 J. Jo, S.-S. Kim, S.-I. Na, B.-K. Yu and D.-Y. Kim, *Adv. Funct. Mater.*, 2009, **19**, 866–874.
11 M. Campoy-Quiles, T. Ferenczi, T. Agostinelli, P. G. Etchegoin, Y. Kim, T. D. Anthopoulos, P. N. Stavrinou, D. D. C. Bradley and J. Nelson, *Nat. Mater.*, 2008, **7**, 158–164.
12 G. Li, V. Shrotriya, Y. Yao, J. Huang and Y. Yang, *J. Mater. Chem.*, 2007, **17**, 3126–3140.
13 H. Hoppe and N. S. Sariciftci, *J. Mater. Chem.*, 2006, **16**, 45–61.
14 T. Kirchartz, K. Taretto and U. Rau, *J. Phys. Chem. C*, 2009, **113**, 17958–17966.
15 O. V. Mikhnenko, H. Azimi, M. Scharber, M. Morana, P. W. M. Blom and M. A. Loi, *Energy Environ. Sci.*, 2012, **5**, 6960–6965.
16 K. S. Nalwa, J.-M. Park, K.-M. Ho and S. Chaudhary, *Adv. Mater.*, 2011, **23**, 112–116.
17 J. B. Kim, P. Kim, N. C. Pegard, S. J. Oh, C. R. Kagan, J. W. Fleischer, H. A. Stone and Y.-L. Loo, *Nat. Photonics*, 2012, **6**, 327–332.
18 D. Duche, P. Torchio, L. Escoubas, F. Monestier, J.-J. Simon, F. Flory and G. Mathian, *Sol. Energy Mater. Sol. Cells*, 2009, **93**, 1377–1382.
19 H. Shen, P. Bienstman and B. Maes, *J. Appl. Phys.*, 2009, **106**, 073109.
20 J. D. Myers, W. Cao, V. Cassidy, S.-H. Eom, R. Zhou, L. Yang, W. You and J. Xue, *Energy Environ. Sci.*, 2012, **5**, 6900–6904.
21 J.-M. Park, Z. Gan, W. Y. Leung, R. Liu, Z. Ye, K. Constant, J. Shinar, R. Shinar and K.-M. Ho, *Opt. Express*, 2011, **19**, A786–A792.
22 T.-Y. Chu, S. Alem, P. G. Verly, S. Wakim, J. Lu, Y. Tao, S. Beaupre, M. Leclerc, F. Belanger, D. Desilets, S. Rodman, D. Waller and R. Gaudiana, *Appl. Phys. Lett.*, 2009, **95**, 063304.
23 Z.-Y. Li and L.-L. Lin, *Phys. Rev. E: Stat., Nonlinear, Soft Matter Phys.*, 2003, **67**, 046607.
24 Z. Ye, X. Hu, M. Li, K.-M. Ho and P. Yang, *Appl. Phys. Lett.*, 2006, **89**, 241108.
25 ISU, ISU TMM Photonic Software Package, http://www.techtransfer.iastate.edu/en/for_industry/technology_search/search.cfm?fuseaction = technology.details&id = 3336.
26 J. D. Kotlarski, P. W. M. Blom, L. J. A. Koster, M. Lenes and L. H. Slooff, *J. Appl. Phys.*, 2008, **103**, 084502.
27 C. M. Ramsdale and N. C. Greenham, *J. Phys. D: Appl. Phys.*, 2003, **36**, L29.
28 H. Hoppe, N. S. Sariciftci and D. Meissner, *Mol. Cryst. Liq. Cryst.*, 2002, **385**, 113–119.
29 Y. Sun, C. J. Takacs, S. R. Cowan, J. H. Seo, X. Gong, A. Roy and A. J. Heeger, *Adv. Mater.*, 2011, **23**, 2226–2230.

